Functional segmentation of dynamic nuclear images by cross-Ψ_B-energy operator

Abdel-Ouahab Boudraa[a,], Jean-Christophe Cexus[a], Habib Zaidi[b]*

[a] IRENav, Ecole Navale, Lanvéoc Poulmic, BP600, 29240 Brest-Armées, France
[b] Geneva University Hospital, Division of Nuclear Medicine, CH-1211 Geneva, Switzerland

ARTICLE INFO

ABSTRACT

We describe a new segmentation method of dynamic nuclear medicine images based on the cross-Ψ_B-energy operator. Ψ_B is a nonlinear measure which quantifies the interaction between two time-signals including their first and second derivatives. Similarity measure, noted SimilB, between the time activity curve (TAC) of each pixel and the mean value of the TACs of a reference region of the scintigraphic image series is calculated. The resulting SimilB map is a functional image representing regions with different temporal dynamics. Some new properties of Ψ_B are presented. Particularly, we show that Ψ_B as a similarity measure is robust to both scale and time shift. The proposed method is applied to nuclear cardiac sequences for visualization and analysis of the ventricular emptying pattern, which may be useful in studying motion or conduction abnormalities. Results of a normal subject and four patients with abnormal ventricular contraction patterns are presented to highlight the suitability of this operator for studying non-stationary TAC series.

© 2006 Elsevier Ireland Ltd. All rights reserved.

1. Introduction

Gated blood pool scintigraphy can measure the functional changes in tissues. This modality generates images demonstrating temporal changes in radioactive tracer distribution. For example, gated blood pool scintigraphy is a reliable non-invasive method for detecting abnormalities of contraction and conduction of the heart [1]. Dynamic imaging provides a time sequence of images taken throughout the whole cardiac cycle. To each image pixel correspond a time-series or a time activity curve (TAC). The images demonstrate temporal changes in radioactive tracer distribution. The quantitative information contained in the images describes the physiological behavior of heart imaged structures such as the left ventricle (LV) and the right ventricle (RV). Classical analysis of such images is performed by visual evaluation of the differences between two consecutive images to obtain qualitative

information about the cardiac contraction kinetics. This is not an optimal way to interpret the changes appearing in the images along the cardiac sequence. Thus, image processing techniques designed to extract as much biomedical/diagnostic information as possible and to ease clinical interpretation have been developed [2,3]. Based on the first harmonic fit to the TAC, Fourier analysis has been used to detect and describe wall motion abnormalities [2,4]. This analysis assumes that the data are periodic and that the transition between the first and the last frame (image) of the cardiac sequence is smooth. The generated phase image corresponds to the time of maximal contraction (end-systole). The phase image allows good separation of the ventricular regions from the atria and this processing is useful to delineate automatically the LV edges in order to estimate the ejection fraction value [5]. However, Fourier analysis has some limitations. The absolute times indicated by the first harmonic phase do not correspond to

---

the onset of contraction but to the end of contraction. Furthermore, the phase is influenced by the shape of the entire TAC. In spite of the apparent mathematical difficulties, factor analysis has gained clinical acceptance for cardiac studies at equilibrium with abnormalities of both contraction and conduction [6]. This analysis supposes that any TAC is a weighted sum of a limited number of pure time activity evolutions (physiological components) [2]. These estimated components, corresponding to regions of similar temporal behavior, are used to construct factor images. While Fourier analysis is based on sine or cosine functions, no such restriction is placed on the shape of the principal components. Although factor analysis provides a valid representation of wall motion and conduction abnormalities, some limitations must be considered. The quality of results obtained by the factor analysis and the number of significant factors depend on the signal to noise ratio of the cardiac sequence. Furthermore, the criteria used for the interpretation must be defined [6,7]. This perhaps avoids the need to make conclusions based on TACs of "non-physiologic" shape. Similarity maps have been used to segment and analyze dynamic MRI data [8], oncological PET image [9], and nuclear cardiac images [3]. This latter reference proposes a similarity measure method based on the covariance function to analyze nuclear cardiac images. Compared to Fourier analysis, this method does not assume that the data are periodic and no restriction is placed on the shape of the pixel TAC. This method segments the TACs of the cardiac images in regions of similar temporal behavior (components) but, contrary to factor analysis the knowledge of the number of components is not required. The similarity approach is based on computing the covariance function between mean TACs of a reference Region of interest (ROI) and the TAC of each pixel of the sequence. The generated covariance map is a representation of the temporal similarity of the pixels to the fixed reference [3]. This method gives good results in cardiac image analysis. However, based on the covariance coefficient (Cov), or the cross correlation (CC), the similarity measure is not necessarily coherent with the TAC shape and does not consider the order of time points and uneven sampling intervals. Furthermore, the Cov (or CC) function is a linear measure and does not include temporal information and the relative changes of the TACs. In this paper, we introduce a new similarity measure denoted SimilB, which includes the temporal information and relative change of the TAC. SimilB is based on the Ψ_B operator the cross [10] a nonlinear function which measures the interaction between two time-signals including their first and second derivatives. Furthermore, the link established between the cross-Ψ_B-energy operator and the cross-Wigner-ville distribution shows that a similarity measure based on this operator is well suited to study non-stationary time series such as TACs.

2. The Ψ_B operator

To measure the interaction between two real time signals the cross Teager–Kaiser operator (CTKEO) has been defined [11]. This operator has been extended to complex-valued signals noted $\Psi_{\mathbb{C}}$, in Ref. [10]. The CTKEO, applied to signals $x(t)$ and $y(t)$, is given by $[x, \dot{y}] \equiv \dot{x}y - x\dot{y}$ where $[x, \dot{y}]$ is the Lie bracket which measures the instantaneous differences in the relative

rate of change between x and $\dot{y}$. In the general case, if x and y represent displacements in some generalized motions, $[x, \dot{y}]$ has dimensions of energy (per unit mass), and is viewed as a cross-energy between x and y [11]. Based on $\Psi_{\mathbb{C}}$ function, a symmetric and positive function, called cross-Ψ_B-energy operator is defined [10]. Let x and y be two complex signals, Ψ_B is defined as [10]:

$$\Psi_B(x, y) = \frac{1}{2}[\Psi_{\mathbb{C}}(x, y) + \Psi_{\mathbb{C}}(y, x)] \tag{1}$$

$$\Psi_B(x, y) = \frac{1}{2}[\dot{x}^*\dot{y} + \dot{x}\dot{y}^*] - \frac{1}{4}[x\ddot{y}^* + x^*\ddot{y} + y\ddot{x}^* + y^*\ddot{x}] \tag{2}$$

where $\Psi_{\mathbb{C}}(x, y)$ is defined by [10]:

$$\Psi_{\mathbb{C}}(x, y) = \frac{1}{2}[\dot{x}^*\dot{y} + \dot{x}\dot{y}^*] - \frac{1}{2}[x\ddot{y}^* + x^*\ddot{y}] \tag{3}$$

$\dot{x}(t)(\dot{y}(t))$, $\ddot{x}(t)(\ddot{y}(t))$ are the first and the second derivatives of $x(t)$ $(y(t))$, respectively. $x^*(t)(y^*(t))$ is the conjugate of $x(y)$. $\Psi_B(x, y)$ is the symmetric bilinear form and $\Psi_B(x, x)$ is the associated quadratic form [10]. $\Psi_B(x, y)$ of complex signals x and y is equal to the sum of their real and imaginary parts [10]:

$$\Psi_B(x, y) = \Psi_B(x_r, y_r) + \Psi_B(x_i, y_i) \tag{4}$$

where $x(t) = x_r(t) + jx_i(t)$ and $y(t) = y_r(t) + jy_i(t)$ and j denotes the imaginary unit. According to (4) the $\Psi_B(x, y)$ is a real quantity, as expected for an energy operator. To compute the analytic signals $x(t)$ or $y(t)$, we use the Hilbert transform. Let $x_r(t)$ and $y_r(t)$ be two real signals, and $x(t)$ and $y(t)$, respectively, their corresponding analytic signals: $x(t) = x_r(t) + jH(x_r(t))$ and $y(t) = y_r(t) + jH(y_r(t))$, where $H(.)$ is the Hilbert transform.

3. Properties of Ψ_B

We provide here some new properties of Ψ_B [10]. We denote Ψ_B of $x(t)$ and $y(t)$ by $\Psi_B(x, y; t)$ and denote by "←" the affectation operation.

- Similarity measure

  $$\Psi_B(x, y; t) = \Psi_B(y, x; t)$$

  This is a basic requirement for most of similarity or distance measures.
- Time-shift

  $$x_1(t) \leftarrow x(t - t_0), \qquad y_1(t) \leftarrow y(t - t_0)$$

  It is trivial that Ψ_B is time-shift invariant, i.e. $\Psi_B(x_1, y_1; t) = \Psi_B(x, y; t - t_0)$. This property states that any time translations in the signals, $x(t)$ and $y(t)$, should be preserved in their measure of interaction, $\Psi_B(x, y; t)$. Thus, $\Psi_B(x, y; t)$ is robust to time shifts.
- Amplitude-scale

  $$x_1(t) \leftarrow \alpha x(t), \qquad y_1(t) \leftarrow \beta y(t)$$

  It is easy to verify that $\Psi_B(x_1, y_1; t) = \alpha\beta\Psi_B(x, y; t)$. Thus, the time where Ψ_B peaks, corresponding to the maximum

of interaction between $x(t)$ and $y(t)$, is robust to amplitude scale.

- Time-scale

$$x_1(t) \leftarrow x(at), \qquad y_1(t) \leftarrow y(at)$$

It is easy to verify that $\Psi_B(x_1, y_1; t) = a^2 \Psi_B(x, y; t)$. This property states that if the time of the two signals is compressed by a scale a, then the energy of interaction is compressed by a^2.

3.1.   Discrete version of Ψ_B

To discretize Eq. (2) time derivatives are approximated by time differences. It is easy to see that both the two-sample forward or backward differences give the same discrete version of Eq. (2), Ψ_B, noted Ψ_{Bd}:

$$\Psi_{Bd}(x_k(n), y_k(n)) = x_k(n)y_k(n) - 0.5[x_k(n+1)y_k(n-1)$$
$$+ y_k(n+1)x_k(n-1)], \quad k \in \{i, r\} \tag{5}$$

where "r" and "i" indicated the real and the imaginary parts. $x_k(n)$ and $y_k(n)$ are the discrete-time signals of their continuous counterparts $x(t)$ and $y(t)$, respectively. t is replaced by $nT_s (n \in \mathbb{N})$ and T_s is the sampling period. Thus, we replace $x(t)(y(t))$ with $x(nT_s)(y(nT_s))$ or simply $x(n)(y(n))$. The astute technical reader will note that the discrete version of $\Psi_B(x, y)$ can be written in the form

$$\Psi_{Bd}(x(n), y(n)) = \Psi_{Bd}(x_r(n), y_r(n)) + \Psi_{Bd}(x_i(n), y_i(n)) \tag{6}$$

An important aspect of Ψ_{Bd} is that it is nearly instantaneous. This is because only three samples are required for the interaction measure computation at each time instant. This excellent time resolution provides us with the ability to capture the interaction energy fluctuations.

3.2. Ψ_B-based similarity measure

A similarity measure $S(x(t), y(t))$ is a function used to compare the TACs $x(t)$ and $y(t)$. Conventionally, this measure is a symmetric function whose value is large when x and y are somehow "similar". The proposed similarity measure based on $\Psi_B(x, y)$, between $x(t)$ and $y(t)$ uses their interaction. A larger value indicates more interaction in energy between TACs [12,13]. If the input variables (or samples) of the TAC $x(t)$ (or $y(t)$) have a large range, then this can overpower the other input variables of $y(t)$ (or $x(t)$). Therefore, the proposed similarity measure, SimilB, is a normalized version of $\Psi_B(x, y)$ and is defined as follows:

$$\text{SimilB}_{xy} = \frac{\sqrt{2} \int_T \Psi_B(x, y) \, dt}{\int_T \sqrt{\Psi_B^2(x, x) + \Psi_B^2(y, y)} \, dt} \tag{7}$$

T is the TAC duration. The similarity is symmetric when comparing two TACs:

$$\text{SimilB}_{xy} = \text{SimilB}_{yx} \forall (x, y) \in \mathbb{C}^2 \tag{8}$$

It is a basic requirement for most of similarity or distance measures. Note that if $x = y$ then $\text{SimilB}_{xy} = 1$.
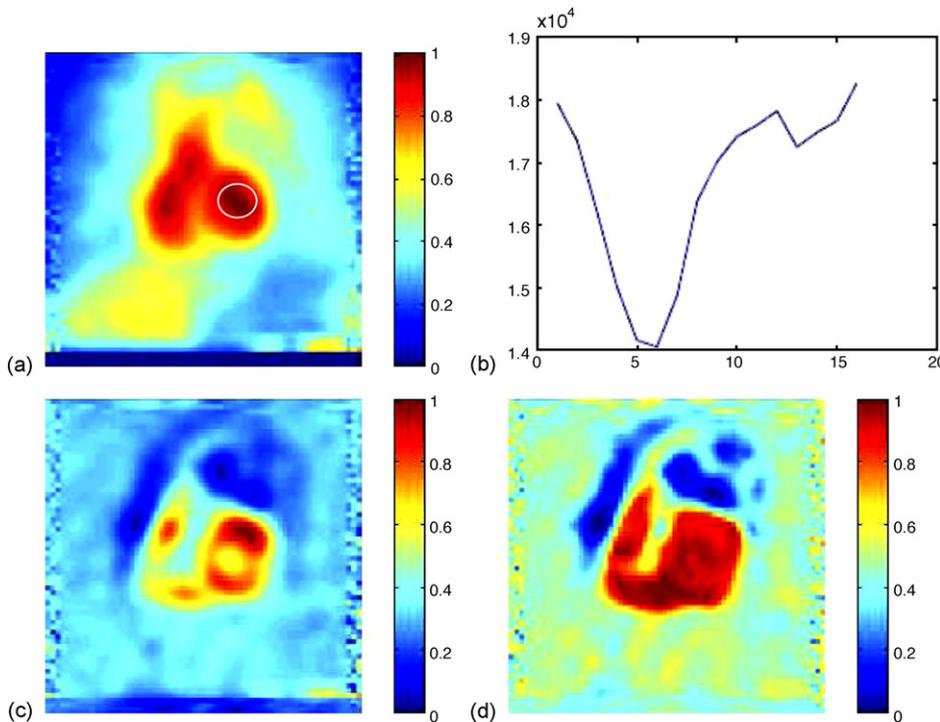

Fig. 1 – Nuclear cardiac image analysis of Patient 1 using ROI$_1$. Cardiac image (a), ROI$_1$ TAC (b), CC image (c), and SimilB image (d).

4. Results and discussion

We illustrate the SimilB with real TACs of five patients (a normal subject (Patient 1) and four patients with abnormal ventricular contraction patterns) derived from gated blood pool imaging method. Equilibrium scintigrams are obtained after injection of 550–740 MBq (15–20 mCi) of Tc-99 m in vivo labeled red blood cells. This imaging technique provides a time sequence of images taken throughout the whole car-
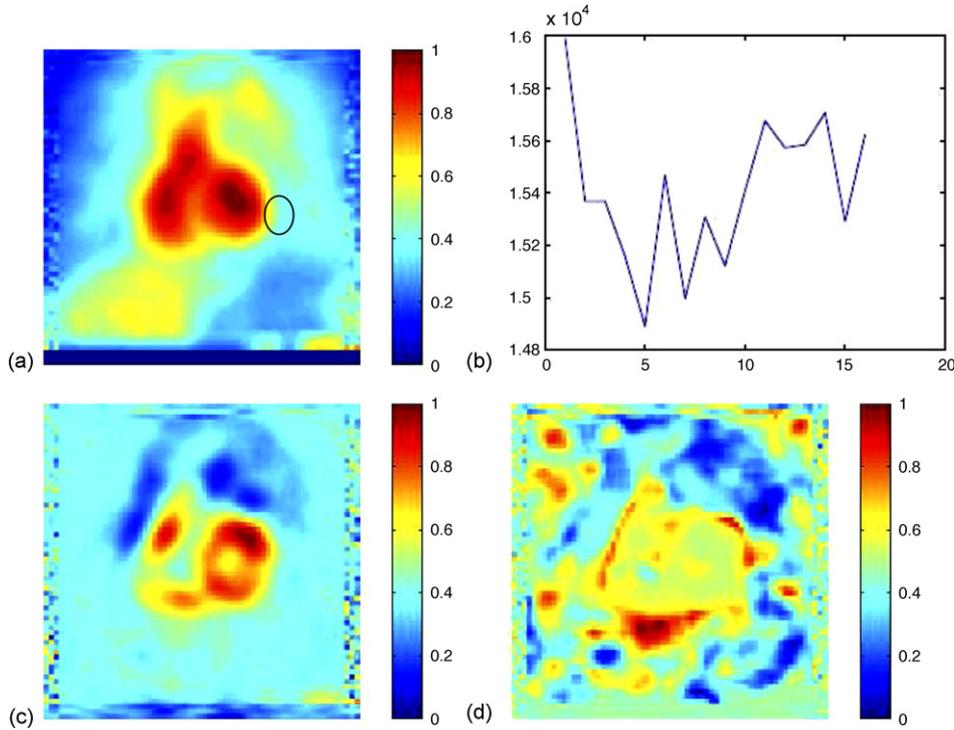

Fig. 2 – Nuclear cardiac image analysis of Patient 1 using ROI$_2$. Cardiac image (a), ROI$_2$ TAC (b), CC image (c), and SimilB image (d).
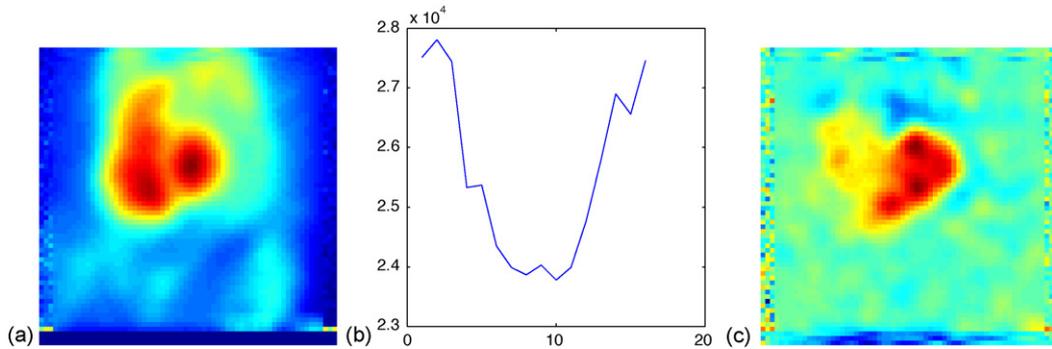

Fig. 3 – Nuclear cardiac image analysis of Patient 2. Cardiac image (a), ROI$_3$ TAC (b), and SimilB image (c).
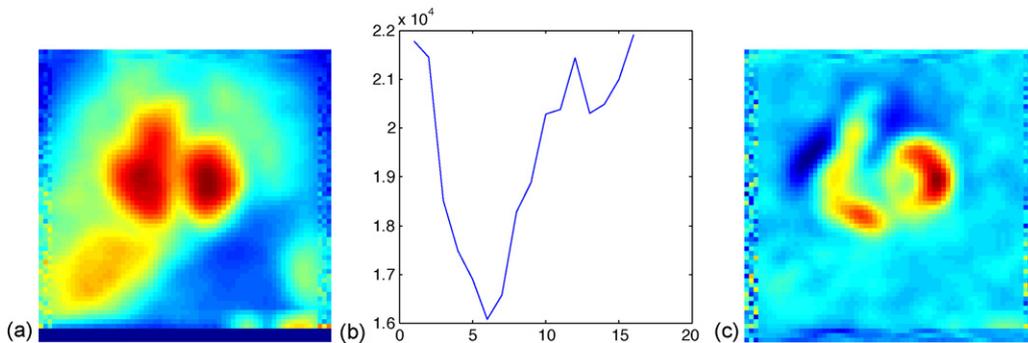

Fig. 4 – Nuclear cardiac image analysis of Patient 3. Cardiac image (a), ROI$_4$ TAC (b), and SimilB image (c).
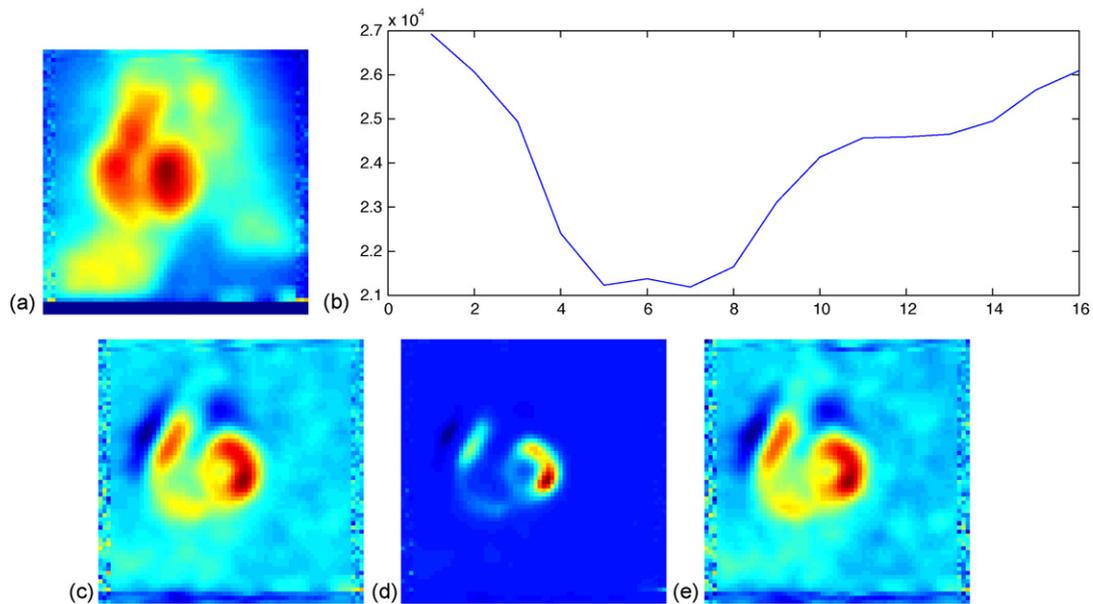
Fig. 5 – Nuclear cardiac image analysis of Patient 4. Cardiac image (a), ROI TAC (b), CC image (c), CS image (d), and SimilB image (e).

diac cycle. Fig. 1(a) (or Figs. 2(a)–6(a)) shows the end diastolic image of the series where the LV region has the largest area. For each pixel of the image corresponds a TAC. The image size is 64×64 which corresponds to 4096 TACs. The cardiac cycle is divided into 16 images. The analysis of these images consists in computing, pixel by pixel, the SimilB between two TACs representing the TAC of any pixel of the sequence and a reference ROI. To compute the complex version of the TACs, the Hilbert transform is used [14]. The generated similarity map is an image where the value of each pixel represents the degree of temporal similarity to the reference (Figs. 1(c and d), 2(c and d), 3(c), 4(c) and 5(c, d and e) and

6(c,d and e)). Two TAC ROIs, denoted ROI_1 and ROI_2, taken, as references on the end diastolic image (Figs. 1(a) or 2(a)) are shown in Figs. 1(b) and 2(b), respectively. ROI_1 and ROI_2 are placed inside and outside of the LV, respectively. Fig. 1(b) represents a typical physiological TAC of the LV. Results of CC and SimilB measures corresponding to ROI_1 and ROI_2 TAC references are illustrated in Figs. 1(c and d) and 2(c and d), respectively. SimilB and CC images are displayed with a 256 color look-up table where each color corresponds to the temporal degree of similarity. For all reference ROI placements, the red color corresponds to a maximum similarity value and the blue color to a minimum one. Thus, in an image region having
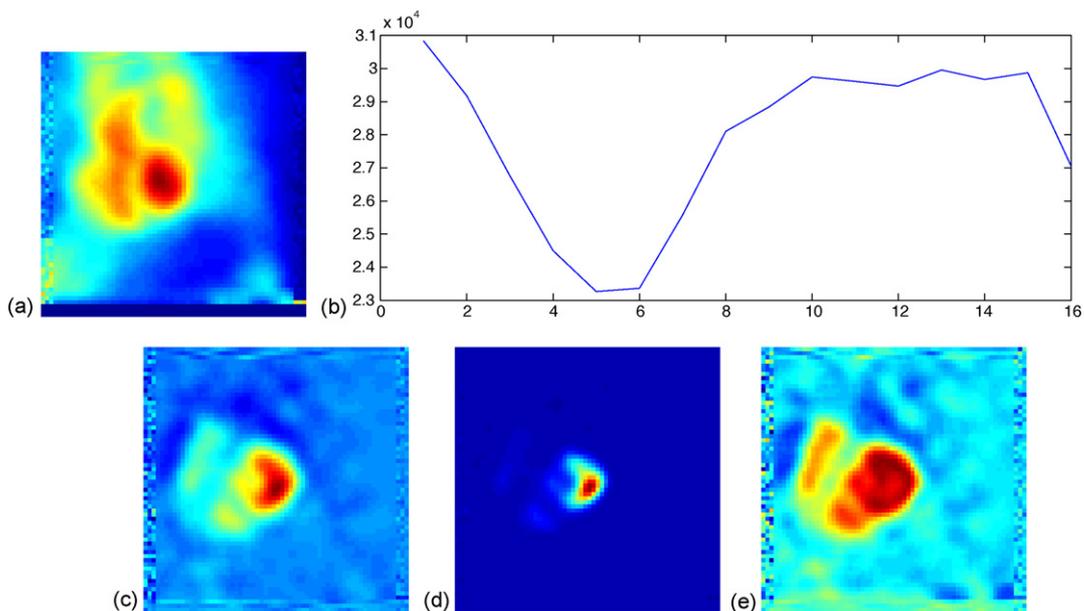

Fig. 6 – Nuclear cardiac image analysis of Patient 5. Cardiac image (a), ROI TAC (b), CC image (c), CS image (d), and SimilB image (e).

the same temporal evolution, the pixels have the same color. For example, the LV and the RV are displayed in red and the atria in blue (Figs. 1(c and d) and 2(c and d)). This is expected since the atrial pixels are out of phase with the ventricular ones. Both SimilB and CC separate the LV and the RV from the atria (Figs. 1(c and d) and 2(c and d)). However, these temporal regions are much better separated by SimilB (Fig. 1(d)) than by the CC (Fig. 1(c)). Furthermore, the CC measure gives the same result (Fig. 1(c) and 2(c)) for two different references (Fig. 1(b) and 2(b)). Results obtained by SimilB are expected since ROI$_2$ TAC does not correspond to physiological TAC and consequently does not carry out meaningful similarity information (Fig. 2(d)). Figs. 3 and 4 show the results obtained in two pathological patients (Patients 2 and 3) where the TAC references are placed on the left ventricular region. In Fig. 3(c) SimilB reveals a high hypokinesis and a low hypokinesis of the inferior and the anterior parts of the RV respectively. One may also note a moderate hypokinesis of the septal segment of the LV. In Fig. 4, SimilB shows a moderate akinesis of the septal segment of the LV and a moderate hypokinesis of the anterior part of the RV. Figs. 5 and 6 show results of comparison of SimilB, in patients 5 and 6, to the CC and to the Cubed sum coefficient (CS) recently introduced by Thireou et al. [9]. It has been reported that the CS gives the best results as a similarity measure in the evaluation of oncological dynamic positron emission tomography images [9]. In both Figs. 5 and 6, end diastolic image (Figs. 5(a) and 6(a)) and chosen ROI TAC (Figs 5(b) and 6(b)) are presented. For Patient 4 (Fig. 5), both CC (Fig. 5(c)) and SimilB (Fig. 5(e)) reveal an anteroseptal and inferoseptal hypokinesia, and also an hypokinesis of the anterior part of the RV. We globally find the same result in CS image (Fig. 5(d)) but the severity or the intensity of cardiac abnormalities is lost or difficult to be assessed. In Patient 5 (Fig. 6), SimilB map shows an hypokinesis of the inferior part of the RV and a moderate hypokinesis of the anterior part of the RV (Fig. 6(e)). These results are confirmed by other clinical investigations. Note that CC map reveals an akyinesie of the RV and moderate hypokinesis of the septal segment of the LV (Fig. 6(c)). As in Patient 4, the CS measure does not permit to assess the severity of the cardiac abnormalities. Furthermore, the opposition of the temporal responses of the ventricles and the atria is not well demonstrated by the CS measure (Figs. 5(d) and 6(d)).

5. Conclusion

Similarity measures such as the CC (or Cov), the CS or the Euclidean distance are not able to capture the temporal information of the TAC. Relative change of amplitude and the corresponding temporal information are well suited to measure similarity between TACs. In this paper, a new functional segmentation method of nuclear cardiac images based on SimilB similarity measure is proposed. This new similarity measure for TACs analysis takes into account the temporal information. Indeed, SimilB uses the first and the second derivatives of the TAC to capture the temporal information. Results obtained in one normal subject and four patients with cardiac abnormalities have shown the advantages of including the derivatives of the TAC and that SimilB resulted in better performance than the CC and the CS measures. SimilB clearly separates

the atria from the ventricles. In the four patients with wall motion abnormalities, areas of various contraction abnormalities are recognized and their boundaries delimited. To confirm the obtained results, a large class of TACs datasets (various pathological cases) must be studied to show the reliability of SimilB for routine clinical use. Furthermore, the obtained results must be compared to methods, other than the CC or the CS, particularly those including the temporal information of the TAC. As the Ψ_B expression involves derivatives of the TAC, it should be noted that the second derivative measure is by nature more sensitive to noise than that of the first derivative. Consequently, SimilB may be sensitive to noise. The TACs studied in this work are not very noisy and thus the obtained results are moderately affected by noise. Note that other similarity measures based on the cross-Ψ_B-energy operator can be constructed or adapted to a given application. As future work, we plan to study the robustness of derivative measures against noise. Also, we plan to investigate the use of SimilB for dynamic PET or MRI studies.

references

[1] S.A. Jackson, R. Nickerson, R.H. Martin, S. Lies, D. Barnes, Regional observer performance variations in the evaluation of gated cardiac blood pool studies, Eur. J. Nucl. Med. 19 (1992) 254–257.

[2] A.O. Boudraa, H. Zaidi, Image segmentation techniques in nuclear medicine, in: H. Zaidi (Ed.), Quantitative Analysis in Nuclear Medicine Imaging, Springer, New York, 2005, pp. 308–357.

[3] A.O. Boudraa, J. Champier, M. Djebali, F. Behloul, A. Beghdadi, Analysis of dynamic nuclear cardiac images by covariance function, Comput. Med. Imag. Graphics 23 (1999) 181–191.

[4] E. Botvinick, R. Dunn, M. Frais, W. O'Connell, D. Shosa, R. Herfkens, M. Scheinman, The phase image: its relationship to patterns of contraction and conduction, Circulation 65 (1982) 551–560.

[5] A.O. Boudraa, J.J. Mallet, J.E. Besson, S.E. Bouyoucef, J. Champier, Left ventricle automated detection method in gated isotopic ventriculography using fuzzy clustering, IEEE Trans. Med. Imag. 12 (1993) 451–465.

[6] F. Cavailloles, J.P. Bazin, D. Pavel, E. Olea, M. Faraggi, F. Frouin, R. Di Paola, Comparison between factor analysis of dynamic structures and Fourier analysis in detection of segmental wall motion abnormalities: a clinical evaluation, Int. J. Cardiac Imag. 11 (1995) 263–272.

[7] M. Fraggi, F. Cavailloles, P. Assayag, F. Benslimene, J.P. Bazin, Evaluation des performances de trois méthodes de traitement de l'image scintigraphique de ventriculographie cardiaque à l'équilibre, J. Biophys. Biomécanique 12 (1986) 67–69.

[8] J. Rogowska, G.L. Wolf, Temporal correlation images derived from sequential MR scans, J. Comput. Assist. Tomogr. 16 (1992) 784–788.

[9] T. Thireou, G. Kontaxakis, L.G. Strauss, A. Dimitrakopoulou-Straus, S. Pavlopoulos, A. Santos, Feasibility study of the use of similarity maps in the evaluation of oncological dynamic positron emission tomography images, Med. Biol. Eng. Comput. 43 (2005) 23–32.

[10] J.C. Cexus, A.O. Boudraa, Link between cross-Wigner distribution and cross-Teager energy operator, IEE Electron. Lett. 40 (12) (2004) 778–780.

[11] P. Maragos, A. Potamianos, Higher order differential energy operators, IEEE Sig. Proc. Lett. 2 (8) (1995) 152–154.

[12] A.O. Boudraa, J.C. Cexus, K. Abed-Meriam, Z. Saidi, Interaction measure of AM-FM signals by cross-Ψ_B-energy operator, in: Proceedings of the IEEE ISSPA, Sydney, Australia, 2005, pp. 775–778.

[13] A.O. Boudraa, J.C. Cexus, F. Salzenstein, A. Beghdadi, Analysis of nuclear time activity curve by cross-Ψ_B-energy operator, in: Proceedings of the IEEE ISCCSP, Marrakech, Morocco, 2006, 4 pages.

[14] D. Gabor, Theory of communication, J. IEE 93 (III) (1946) 429–457.